3RD CAJG 2020

Estimating and mapping evapotranspiration in olive groves of semi-arid Tunisia using empirical formulas and satellite remote sensing

Amani Bchir[1] · Soumaia M'nassri[2] · Saoussen Dhib[3] · Asma El Amri[2] · David Mulla[4]

Abstract

Accurate estimation of evapotranspiration (ET) is needed to optimize irrigation in semi-arid environments. The present work aims to estimate evapotranspiration using empirical formulas and remote sensing in a commercial olive orchard near Menzel Mhiri in east central Tunisia. This study compares evapotranspiration with the Mapping Evapotranspiration at high Resolution with Internal Calibration (METRIC) model with estimates from five empirical equations (Penman–Monteith; Blaney-Criddle; Hargreaves temperature; Hargreaves radiation; and Priestley-Taylor). Reference evapotranspiration estimated using these five empirical equations was based on meteorological station measurements in olives at the pilot study site. Three years of ET estimates based on Landsat-8 satellite images and the METRIC method covering 2017, 2018, and 2019 were downloaded using Google EEFlux.

The results obtained by remote sensing showed good ability to characterize seasonal variation in reference (ET_0) and actual crop (ETc) evapotranspiration. Reference evapotranspiration values for olive trees estimated by the METRIC model during the three experimental years accurately represent those estimated with the Penman–Monteith formula. Also, there was very good agreement between results obtained with METRIC and those calculated using the Blaney-Criddle method. The monthly average of ET_0 and ETc values determined during the three experimental years (2017, 2018, and 2019) showed that the METRIC model underestimates irrigation needs by about 15% compared to the Penman–Monteith (PM) approach.

Introduction

Many regions around the world have been severely impacted by extensive droughts associated with climate change over the last two decades, particularly on the African continent. Water resources are adversely impacted by global warming (Nyenjie and Batelaan 2009). In Africa, the water crisis is one of the main factors limiting agricultural development (Lian and Huang 2016). According to Amazirh et al. (2017), water scarcity is likely to be exacerbated in the near future by the alterations in the hydrological cycle associated with climate change as well as by increased demand for water in agriculture. As a result, improved irrigation water management is critical for protecting and conserving water resources.

Located on the southern shore of the Mediterranean, Tunisia experiences arid and semi-arid climates, water resources are limited and variable in time and space, and

✉ Amani Bchir
  ameni.bchir@gmail.com

[1] Institut de L'Olivier, Sfax, Tunisia

[2] Institut Supérieur Agronomique de Chott- Mariem, Sousse, Tunisia

[3] Department of Atmospheric Physics, Faculty of Mathematics and Physics, Charles University, Prague, Czech Republic

[4] Department of Soil, Water & Climate, University Minnesota, Minneapolis, MN, USA

agriculture faces increasing scarcity of water resources (M'nassri et al. 2019). These factors restrict Tunisia's socioeconomic development, particularly in the agricultural sector. However, olive trees are one of the species best adapted to water scarcity and drought conditions due to their physiological and morphological traits. Perennial olive trees contribute positively to sustainability of Tunisia's agricultural economy (Melaouhi et al. 2021). According to Chebbi et al. (2018), olive orchards cover 1.8 million hectares in Tunisia, with 65 million olive trees accounting for nearly 79% of total tree-covered area and 34% of arable land. Therefore, optimizing irrigation water management for olive orchards is crucial to safeguarding this agroecosystem.

Irrigation water management affects crop evapotranspiration (ET), which is generally the largest component of the water balance, responsible for dissipating up to 60% of rainfall inputs (Ait Hassine et al. 2020). ET depletes soil moisture in arid and semi arid regions (Ortega-Salazar et al., 2021; Alcaras et al. 2021), leading to crop water stress if not accompanied by irrigation to replenish soil moisture. Hence, understanding soil–plant-atmosphere interactions requires accurate estimation of evapotranspiration. A large number of formulas have been used, developed and/or improved to calculate the water consumed in the form of monthly or seasonal reference evapotranspiration (Blaney and Criddle 1950; Priestley and Taylor 1972; Hargreaves and Allen 2003; Temesgen et al. 2005; Popova et al. 2006; Martinez and Thepadia 2010; Todorovic et al. 2013; Razieia and Pereira 2013; Masmoudi-Charfi and Habaieb 2014; Valipour 2017; Landeras et al. 2018; Bchir et al. 2019a; Paredes et al. 2020; Pereira et al. 2020).

Recently, remote sensing tools have been developed to monitor hydrological variables. In particular, remote sensing provides input data for various computational models that estimate crop evapotranspiration (ETc) based on the surface energy balance. This facilitates detection, mapping, and management of crop water stress in irrigated fields. Numerous studies have demonstrated the relevance of remote sensing for estimation of evapotranspiration. For example, French et al. (2015) and Ma et al. (2018) used multi source remote sensing data to estimate evapotranspiration at high spatial resolution and temporal resolution, as well as irrigation water efficiency in order to manage and plan agricultural water resources. Mahmoud and Gan (2019) combined remote sensing with meteorological data to assess spatio-temporal variation of actual evapotranspiration for alfalfa crops in arid regions of the Middle-East. They found good agreement between model estimates and observed daily evapotranspiration. Xue et al. (2020) evaluated remote sensing-based evapotranspiration models such as pySEBAL (a new version of the Surface Energy Balance Algorithm for Land) SEBS (Surface Energy Balance System algorithm), and METRIC (Mapping Evapotranspiration at High Resolution with Internalized Calibration) in almond, tomato, and maize crops. They found that evapotranspiration was accurately estimated with pySEBAL and METRIC, facilitating improved irrigation management during peak crop water demand periods.

Despite the fact that extensive research has been conducted on remote sensing of evapotranspiration, few studies exist on remote sensing of evapotranspiration in semi-arid region olive orchards. Hence, this study aims to assess the feasibility of using satellite remote sensing to estimate spatial and temporal irrigation requirements in Tunisian olive orchards. In addition, this study aims to identify the least complicated and most accurate empirical evapotranspiration calculation method at an experimental olive orchard site in semi-arid Tunisia. To achieve these aims, we compared five empirical ET equations (Penman- Monteith equation (ET_0-PM), Blaney-Criddle (ET_0-BC), Hargreaves temperature (ET_0-HT), Hargreaves radiation (ET_0-HR), and Priestley-Taylor (ET_0-PT) with satellite estimates of ET_0 using METRIC.

Material and methods

Study area

The study area is located in Menzel Mhiri in east central Tunisia, between 35° 25′ 28″ N and 9° 51′ 08″ E. This area covers approximately 377 km² and belongs to the Kairouan region (Fig. 1). Menzel Mhiri is surrounded by Draa Affane in the north, by Siouf-Cherahil in the west, by sabkha of Cherita and Mechertat in the south, and by sabkha Sidi El Hani in the east. The study area lies within a semi-arid climate region. The annual average rainfall is about 320 mm. The monthly average temperature varies between 10 and 28 °C in December and August, respectively. Olive orchards have been intensively planted for the two last decades in this area. In the center of the Menzel Mhiri plain, an commercial olive orchard 0.09 km² in area was equipped with a meteorological station to measure daily average air temperature, minimum air temperature, maximum air temperature, daily average soil temperature at two depths, daily average relative humidity, minimum relative humidity, maximum relative humidity, daily average net radiation, daily average wind speed, and daily average precipitation. The study area has been occupied by olive trees since 2005, with a planting density of 6×6 m.

Reference evapotranspiration (ET_0) estimation using empirical models

Major factors affecting the estimation of reference evapotranspiration include solar radiation, air temperature,
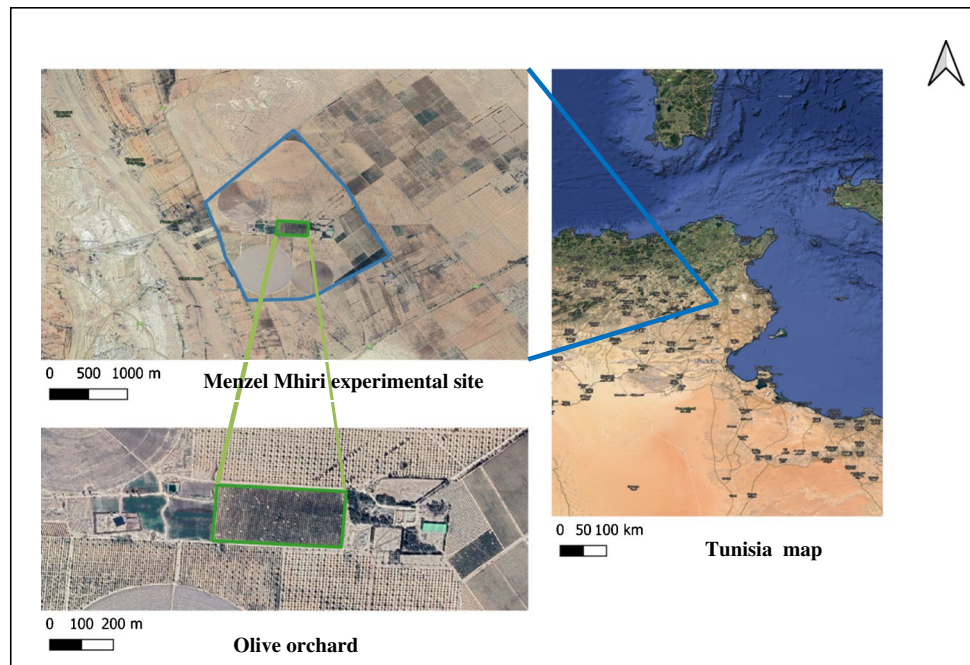
atmospheric water vapor pressure, and wind velocity. These factors were measured using a climatic station established in the study field. The climatic data used in this study covered a period of 3 years, between 2017 and 2019. Reference evapotranspiration is estimated with these data using five empirical models described below.

Many empirical reference evapotranspiration models have been developed in the past. Among these, some require a reasonable number of climatic factors, while other models require a large meteorological dataset of variables which are rarely measured using meteorological stations (Bchir et al. 2019a; Maeda et al. 2011). The models used in this study include Penman–Monteith (PM), Blaney-Criddle (BC), Hargreaves temperature (HT), Hargreaves radiation (HR), and Priestley-Taylor (PT) models. They are described in more detail below:

Penman–Monteith model

The Penman–Monteith method involves climatic parameters such as temperature, water vapor pressure, wind velocity, and solar radiation (Allen et al. 1998). The value of ET_0 is defined by the following equation (Eq. 1):

$$ET_0 = \frac{0.408\Delta\left(R_n - G\right) + \gamma\frac{900}{T+273}U_2(e_a - e_d)}{\Delta + \gamma(1 + 0.34U_2)} \quad (1)$$

where ET_0 refers to reference evapotranspiration (mm/day); R_n denotes the solar radiation at the crop surface (MJ/m^2. day); G represents soil heat flux (MJ/m^2. day); and T is average daily air temperature at 2 m (°C); U_2 denotes

the wind velocity measured at 2 m (m/s); $(e_a - e_d)$ represents vapour pressure deficit (kPa); Δ refers to vapor pressure curve slope (kPa/°C); γ denotes psychrometric constant (kPa/°C); and 0.34 represents wind coefficient (s/m).

Blaney-Criddle model

The Blaney-Criddle method was developed for arid regions of the USA. This model generally provides an accurate estimate of ET_0 (Fooladmand and Ahmadi 2009). The Blaney-Criddle model is used when only precipitation and temperature are measured at a given location. It involves the average daily percentage of annual daytime hours for different latitudes (P) and monthly mean temperature (T). The reference evapotranspiration is estimated by (Blaney and Criddle 1962) using:

$$ET_0 = P \times (0.46T_{mean} + 8) \quad (2)$$

Hargreaves temperature and radiation models

The Hargreaves temperature method has been used worldwide. Its application requires only monthly average, minimum and maximum air temperature data and top of atmosphere radiation (Hargreaves et al. 2003). The reference evapotranspiration ET_0 is defined according to Eq. 3. The Hargreaves radiation method uses only mean solar radiation and daily mean air temperature (Bois et al. 2007). Reference evapotranspiration calculated using the Hargreaves radiation method is estimated using Eq. 4:

$$ET_0 = 0.0023 \times R_A \times TD^{0.5} \times (T + 17.8) \tag{3}$$

$$ET_0 = 0.0135 \times (T_d + 17.8) \times R_s \tag{4}$$

where R_A is top of atmosphere radiation (cal/cm^2 day^1); TD denotes difference between maximum and minimum temperature (°C), T represents monthly average of temperature (°C); T_d and R_s represent daily average temperature (°C) and daily average solar radiation (MJ/m^2).

Priestley-Taylor model

Priestley-Taylor is another empirical model (Priestley and Taylor 1972) for reference evapotranspiration estimated for a large wet surface under minimum advection conditions (Sumner and Jacobs 2005). It is given by the following equation:

$$ET_0 = \propto \frac{\Delta}{\Delta + \gamma} (R_n - G) \tag{5}$$

where $\propto$ denotes an empirical correction, Δ and γ represent slope of the saturated vapor pressure curve and the psychrometric constant, respectively, R_n is solar radiation (W/m^2), and G is soil heat flux (W/m^2).

Reference evapotranspiration (ET_0) estimation using satellite remote sensing

Satellite remote sensing is also used in this study to assess reference evapotranspiration. It is based on the energy balance model known as Mapping Evapotranspiration at high Resolution and with Internalized Calibration (METRIC) (Allen et al. 2007). Landsat 8 satellite images were selected from Earth Engine Evapotranspiration Flux (EEFLux) that operates on the Google Earth Engine system (Allen et al. 2015). EEFlux METRIC algorithms use Level 2 Landsat imagery, which are corrected for top of atmosphere reflectance. EEFLUX was developed by a consortium that includes the University of Nebraska-Lincoln, Desert Research Institute and University of Idaho. EEFlux utilizes the thermal band of Landsat to derive the surface energy balance and short wave bands to estimate vegetation biomass, albedo, and surface roughness. Level 1 of EEFlux employs automated calibration of the image. The list of images available includes an assessment of percent cloud cover for the entire scene as determined by the USGS EROS data center. General equations used for EEFlux, based on METRIC, are summarized by Irmak et al. (2012). All images in this present study were for days having 0% cloud cover at the study site; these were subsequently downloaded from https://eeflux-level1.appspot.com/. Imagery was obtained

from January 2017 to August 2019. Each image was then processed using ArcGIS software version 10.8.

Evaluation of model accuracy

The empirical methods used in this study are evaluated by taking the Penman–Monteith (PM) Equation as a reference, since it has often been demonstrated to be a very accurate method (Fluente-Saiz et al. 2017; Jabloun and Sahli 2008). Accuracy of these empirical models is assessed using standard statistics such as the root mean square error (RMSE) and mean absolute error (MAE) defined by Eqs. 6 and 7, respectively:

$$RMSE = \sqrt{\frac{1}{n} \sum (ET0_{cal} - ET0_{PM})^2} \tag{6}$$

$$MAE = \frac{\sum |ET0_{cal} - ET0_{PM}|}{n} \tag{7}$$

where n denotes the number of observations, ET_{0cal} is the calculated evapotranspiration using the empirical models, and ET_{0PM} is the calculated evapotranspiration using Penman–Monteith.
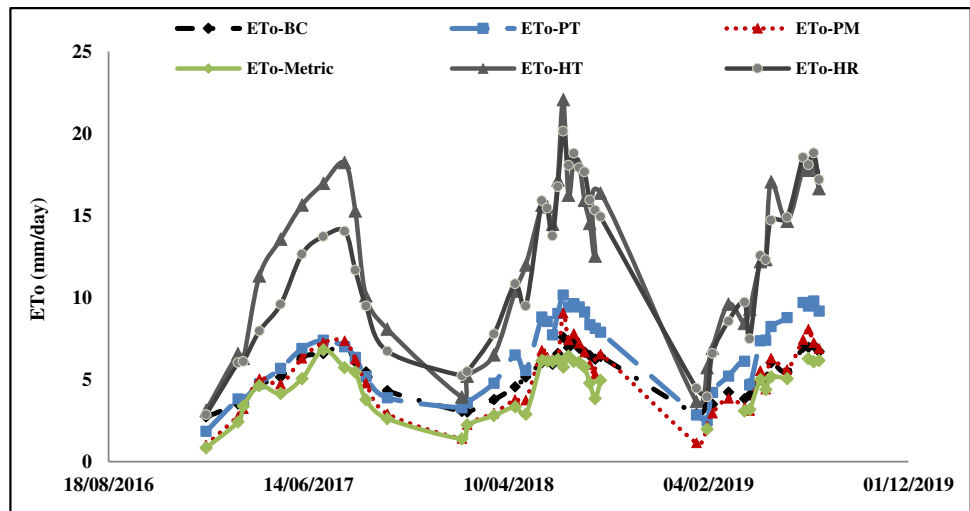
Results

ET_0 estimated using empirical methods

The reference evapotranspiration (ET_0) estimated using the Penman–Monteith (PM), Blaney-Criddle (BC), Hargreaves temperature (HT), Hargreaves radiation (HR), Priestley-Taylor (PT), and METRIC models is shown in Fig. 2. ET_0 values estimated for 2017 to 2019 range from 1.0 to 9.0, from 2.7 to 7.6, from 1.8 to 10.1, and from 0.8 to 6.8 mm/day with the PM, BC, PT, and METRIC methods, respectively. Reference ET_0 varied seasonally, with the lowest values in January and the highest values in July. On average, the ET_0-METRIC, ET_0-BC, and ET_0-PT values were 87.7%, 114.7%, and 136.2%, respectively, of the ET_0-PM values. However, the ET_0 values estimated with the HT and HR methods are much larger than the values estimated with the other methods. ET_0 varies between 3.1 to 22.1 and 2.8 to 20.1 mm/day using the HT and HR methods, respectively, from 2017 to 2019. HT and HR equations overestimated ET_0 (by 250.1% and 239.3% relative to the ET_0-PM values, respectively), especially during periods of high evaporative demand.

Regression lines between reference ET_0 values averaged over three years from the BC, PT, and METRIC methods relative to values with the PM method are shown in Fig. 3. This comparison is limited to the three models cited, because HT and HR greatly overestimate
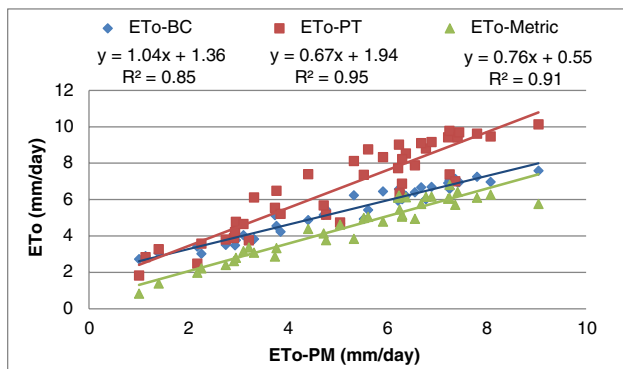
Fig. 2 Reference evapotranspiration (ET_0, mm/day) values estimated at Menzel Mhiri olive orchard by several methods: Penman–Monteith (ET_0-PM), Blaney-Criddle (ET_0-BC), Hargreaves temperature (ET_0-HT), Hargreaves radiation (ET_0-HR), Priestley-Taylor (ET_0-PT), and the METRIC model from 2017 to 2019

Fig. 3 Regression lines between ETo averaged over three years from the Blaney-Criddle, Priestley-Taylor, and METRIC models relative to values from the PM model
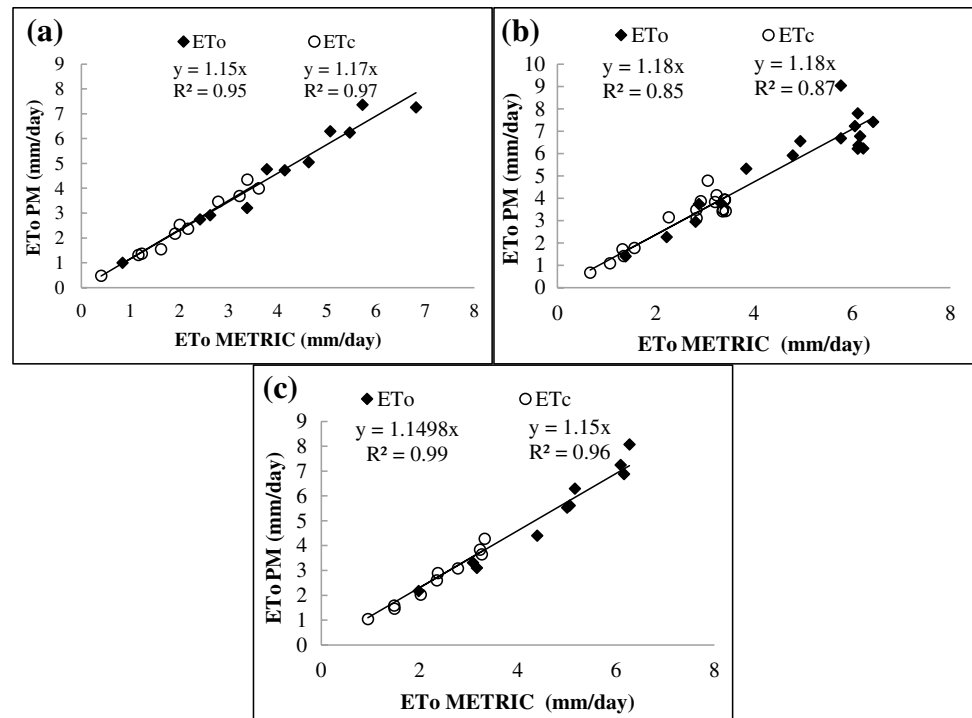

evapotranspiration. Results clearly reveal that the three methods provide accurate estimates, with R^2 values of approximately 0.85, 0.94, and 0.90 for BC, PT, and MET-RIC, respectively. Additionally, *RMSE* values range from 0.79 mm/day with the BC model to 1.82 mm/day with the METRIC model. *MAE* values are approximately 0.64 mm/day with the BC model, 1.03 mm/day with the METRIC model, and 1.52 mm/day with the PT model.

The R^2, *RMSE*, and *MAE* indexes indicate that BC, PT, and METRIC models have good correlation with Penman–Monteith model results, and relatively small statistical errors. Thus, the estimated ET_0 values using BC, PT, and METRIC models are the most appropriate for the present study area, while the HT and HR models are not able to provide accurate values of ET_0 for this region.

ET_0 and ETc estimated using remote sensing techniques

Potential evapotranspiration (ET_0) estimates at the experimental olive orchard using the Penman–Monteith equation for 2017, 2018, and 2019 are strongly correlated with MET-RIC estimates based on satellite data (Fig. 4). R^2 values are above 0.85 in any given year with ET_0-METRIC. Satellite measurements tend to underestimate ET_0 in comparison with the ground-based estimation by about 15% (2017 and 2019) and 18% (2018). This is most likely related to the mixing of crop and bare soil pixels in satellite imagery. Estimates of actual crop evapotranspiration (ETc) using the Penman–Monteith method are also strongly correlated (more than $R^2 = 0.87$) with ETc values estimated using METRIC (Fig. 4).

Estimating irrigation water requirements

The monthly average ET_0 and ETc estimates during the three experimental years (2017, 2018, and 2019) are presented in Table 1. Results are summarized according to a calendar of irrigation water requirements for olive tree phenology that either (a) replenishes 100% ETc using conventional irrigation or (b) replenishes 60% ETc. using deficit irrigation. ET_0 and ETc values are greater for the PM than the METRIC approach. This difference is more important at an annual scale. For ET_0, METRIC underestimates irrigation needs by about 15% compared with the PM approach. The MET-RIC ETc value (555 or 333 mm) is about 13% smaller than the ETc-PM value (641 or 385 mm) for conventional (full) or deficit irrigation, respectively. Deficit irrigation reduces water usage by 40% with the METRIC or PM approaches. Irrigation requirements are the greatest during the months of June, July, and August, corresponding to olive phenological stages of fruit development, core hardening, and fruit

Fig. 4 Correlations between reference and actual crop evapotranspiration (ET_0 and ETc) values, determined using Landsat 8 satellite imagery, versus PM ET_0 based on field weather data for years: **a** 2017, **b** 2018, and **c** 2019

Discussion

Comparison between PM, BC, HT, HR, PT, and METRIC models

A comparison between PM, BC, HT, HR, PT, and METRIC models showed that PM accurately estimates ET_0 and performs better than other models due to its accurate representation of the energy budget. Relative to PM estimates, BC, PT, and METRIC models performed well and had high levels of accuracy in estimating ET_0. Several researchers, including Xiaoying and Erda (2005), Alexandris et al. (2008), Bchir (2015), and Bchir et al. (2019a), used these models and found the PM method was very robust and avoided overfitting. Differences between models increase as the number of climatic factors involved in each formula decreases. Wrachien and Mambretti (2015), Yannopoulos et al. (2015), Khoshravesh et al. (2017), and Valipour (2017) suggested that the most important parameters affecting variations in evapotranspiration are air temperature, humidity, wind speed, and solar radiation. HT and HR models had poor levels of accuracy because they fail to include some of the key climatic variables that affect the energy budget. Several authors previously showed that the HT formula

overestimates ET in humid regions compared to ET_0-PM (Bouhlassa and Paré 2006; Alexandris et al. 2008; Tabari 2010; Martinez and Thepadia 2010; Todorovic et al. 2013; Razieia and Pereira 2013; Bchir et al. 2019a). In the same context, Paredes and Rodrigues (2010) showed that use of the HT equation produced ET values that were less accurate than those estimated by the PM equation. This error is more important in humid regions compared to arid regions. The PT and BC equations are the most accurate ET equations relative to the PM equation for Tunisia in different bioclimatic regions (subhumid, semi-arid, and arid). Masmoudi-Charfi and Habaieb (2014), Bchir (2015), and Bchir et al. (2019a) also found a good correlation between PM and BC models in different bioclimatic regions of Tunisia. Lastly, comparison of the PM and METRIC models showed moderately good correlation. Tasumi (2019) also demonstrated that the METRIC model performed well and had a high level of correlation when compared to the PM method for irrigated crops (apple and grape). However, the METRIC method overestimates ET_0 in non-irrigated bare soil fields.

Relevance of remote sensing techniques

Results of this study show that the METRIC remote sensing method provides accurate temporal estimates for potential ET_0 in Tunisian olive orchards. Elnmer et al. (2019), Pôças et al. (2014), Saadi (2018), and Tasumi (2019) also found similar results. Furthermore, they showed that the METRIC model can be used operationally to estimate and to map ET_0

Table 1 Calendar of water requirements (mm) for two strategies of olive tree irrigation based on the Penman Monteith and METRIC methods for the estimation of ET_0 as a function of phenological olive growth stage

Irrigation strategy	Phenological stage ↓ ET model	Resumption of flowering	Appearance of flower buds	Flowering	Fructification	Fruit development	Core hardening	Fruit growth	Beginning of maturation	Total (mm/year)
	Month	March	April	May	June	July	August		September	
ET_0	ET_0-PM	96.68	118.24	158.52	203.45	238.85	193.51	136.37	87.48	1233.10
	ET_0-METRIC	95.80	120.92	140.98	171.51	192.59	157.70	113.28	81.23	1074.02
ETc (Full Irrigation)	ETc-PM	46.41	55.57	72.92	111.90	126.59	114.17	72.28	41.12	640.95
	ETc-METRIC	45.98	56.83	64.85	94.33	102.07	93.04	60.04	38.18	555.34
Deficit irrigation Dose (60% ETc)	PM	27.85	33.34	43.75	67.14	75.96	68.50	43.37	24.67	384.57
	METRIC	27.59	34.10	38.91	56.60	61.24	55.83	36.02	22.91	333.20

of high density planting olive orchards, with a high correlation of 0.85. ET maps developed using METRIC remote sensing techniques in previous studies provided good spatio-temporal quantification and distribution at high spatial resolution (Numata et al. 2017). These results are consistent with the results of Saadi (2018). Elnmer et al. (2019) compared actual ETc-PM to ETc determined using Landsat-8 images. They found an acceptable estimation of the spatial and temporal distribution of ETc, with R^2 and *RMSE* values of about 0.98 and 0.47 mm/day, respectively. Therefore, the results of the present work show that remote sensing based on satellite images may be used, with adjustments for under-estimation, in order to calculate crop water and irrigation requirements in olive orchards of Tunisia.

Irrigation scheduling for olive orchards

In this study, considerable water savings strategies of up to 40% are possible using deficit irrigation. Using ETc values determined by the PM or the METRIC approaches allows estimation of olive tree water requirements (under either full or deficit irrigation). According to Fernández et al. (2018), in Mediterranean areas, the annual average ET_0 values range between 1200 and 1400 mm, which are similar to the values found in our study. ETc of olive orchards is about 700 mm for a planting density of 100 to 300 trees per ha. Several authors (Fernández et al. 2011, 2013; Elsayed-Farag 2014; López Bernal et al. 2015; Hernandez-Santana et al. 2016; Fernández 2017; Bchir et al. 2019a, 2019b) studied irrigation requirements across a range of irrigation scheduling treatments (e.g. 100%, 70%, 60%, or 35% to 30% of ETc), which are consistent with the two treatments (100% and 60% of ETc) proposed in the irrigation water requirements calendar in Table 1.

Conclusions

Our results showed that ET in a Tunisian olive orchard could be accurately predicted using satellite imagery. ET could also be estimated using empirical equations such as the PM, PT, or BC approaches. The use of the PT equation and/or the BC equation for estimating water requirements is easier than the other equations evaluated in this study when certain climatic parameters (e.g. VPD, wind, R_n) are lacking.

Satellite-based estimates were responsive to temporal variability in climate. The reference evapotranspiration values for olive trees estimated by the METRIC model during the three experimental years were accurate compared to those calculated using the Penman–Monteith formula. The satellite imagery data underestimate ETc measurements by 17%, 18%, and 15% respectively in 2017, 2018, and 2019, so higher resolution imagery is needed to separate bare soil

from vegetated surfaces to improve the utility of METRIC ET estimates. The monthly average of ET_0 and ETc values determined during the three experimental years (2017, 2018, and 2019) showed that the METRIC model underestimates irrigation needs by about 15% compared to the PM approach value. The METRIC ETc value is about 13%, which is less than the ETc-PM value. A fine spatial resolution ET map derived from Landsat 8 will allow users to address certain key issues such as estimating olive tree water status for precision irrigation in Tunisia.

Declarations

Conflict of interest The authors declare no competing interests.

References

Alcaras MA, Peter CR, Searles S (2021) Yield and water productivity response of olive trees (cv Manzanilla) to post-harvest deficit irrigation in a non-Mediterranean climate. Agri Water Manag J 245:106562

Amazirh A, Re-Raki S, Chehbouni A, Rivalland V, Diarra A, Khabba S, Essahar J, Merlin O (2017) Modified Penman-Monteith equation for monitoring evapotranspiration of wheat crop: relationship between the surface resistance and remotely sensed stress index. Biosys Eng J 164:68–84

Alexandris S, Stricevic R, Petkovic S (2008) Comparative analysis of reference evapotranspiration from the surface of rainfed grass in Central Serbia, calculated by six empirical methods against the Penman-Monteith formula. Eur Water 21(22):17–28

Allen R, Pereira L, Raes D, Smith M (1998) Crop Evapotranspiration. Guidelines for computing crop water requirements. FAO Irrigation and Drainage, Paper 56. Food and Agriculture Organization of the United Nations, Rome, 300 p

Allen RG, Tasumi M, Trezza R (2007) Satellite-based energy balance for mapping evapotranspiration with internalized calibration (METRIC)—Model. Irrig Drain Eng J 133:380–394

Allen RG, Morton C, Kamble B, Kilic A, Huntington J, Thau D (2015) EEFlux: a Landsat-based evapotranspiration mapping tool on the Google Earth Engine. In: 2015 ASABE/IA Irrigation Symposium: Emerging Technologies for Sustainable Irrigation-A Tribute to the Career of Terry Howell, Sr. Conference Proceedings (pp. 1–11). Am Soc Agric Biol Eng

Bchir A (2015) Etude de l'évapotranspiration et de la transpiration pour l'estimation des besoins en eau de l'olivier (*Olea europaea* L.) conduit en intensif dans différents étages bioclimatiques. Chott-Mariem: Institut Supérieur Agronomique de Chott- Mariem, 2015. (Thèse de doctorat en Sciences Agronomiques)

Bchir A, Lemeur R, Ben Meriem F, Boukherissa N, Gariani W, Sbaii H, Ben Dhiab A, Ben Mansour Gueddes S, Braham M (2019a) Estimation and comparaison of reference evapotranspiration using different methods to determine olive trees irrigation schedule in different bioclimatic stages of Tunisia. Braz J Bio Sci 6(14):615–628

Bchir A, Mulla DJ, Ben Dhiab A, Ben Meriem F, Bousetta W, Braham. M (2019) Assessing spatial and temporal variability in

evapotranspiration for olive orchards in Tunisia using satellite remote sensing. In: (J. V. Stafford, ed.) Precision Agriculture 19. pp: 431 – 436

Blaney HF, Criddle WD (1950) Determining water requirements in irrigated areas from climatologically and irrigation data. USDA, Washington

Blaney HF, Criddle WD (1962) Determining consumptive use and irrigation water requirements. USDA Technical Bulletin 1275. US Department of Agriclture

Bois B, Pieri P, Van Leeuwen C, Wald L, Huard F, Gaudillere J-P, Saur E (2007) Using remotely sensed solar radiation data for reference evapotranspiration estimation at a daily time step. Agr Forest Meterol J 148:619–630

Bouhlassa S, Paré S (2006) Évapotranspiration de référence dans la région aride de Tafilalet au sud-est du Maroc. Afri J Environ Assess Manam 11:1–16

Chebbi W, Boulet G, Dantec V, Lili Chabaane Z, Fanise P, Mougenot B, Ayri H (2018) Analysis of evapotranspiration components of a rainfed olive orchard during three contrasting years in a semi-arid climate. Agr Forest Meteorol J 256–257

Elnmer A, Khadr M, Kanae S, Tawfik A (2019) Mapping daily and seasonally evapotranspiration using remote sensing techniques over the Nile delta. Agr Water Manag 213:682–692

Elsayed-Farag S (2014) Irrigation scheduling from plant-based measurements in hedgerow olive orchards. University of Seville, pp: 218

Fernández JE (2017) Plant-based methods for irrigation scheduling of woody crops. Horti 3:35. https://doi.org/10.3390/horticulturae3020035

Fernández JE, Moreno F, Martín-Palomo MJ, Cuevas MV, Torres-Ruiz JM, Moriana A (2011) Combining sap flow and trunk diameter measurements to assess water needs in mature olive orchards. Environ Exp Bot 72:330–338

Fernández JE, Perez-Martin A, Torres-Ruiz JM, Cuevas MV, Rodriguez-Dominguez CM, Elsayed-Farag S, Morales-Sillero A, García JM, Hernandez-Santana V, Diaz-Espejo A (2013) A regulated deficit irrigation strategy for hedgerow olive orchards with high plant density. Plant Soil 372:279–295

Fernández JE, Diaz-Espejo A, Romero R, Hernandez-Santana V, García JM, Padilla-Díaz CM, Cuevas MV (2018) Chapter 9 - Precision Irrigation in Olive (Olea europaea L.) Tree Orchards. Water scarcity and sustainable agriculture in semi-arid environment. Tools, Strategies, and Challenges for Woody Crops. 179–217

Fluente-Saiz D, Ortega-Farias S, Fonseca D, Ortega-Salazar S, Kilic A, Allen R (2017) Calibrated of METRIC model to estimate energy balance over a drip-irrigated Apple Orchard. Remote Sens J 9:670–678

Fooladmand HR, Ahmadi SH (2009) Monthly spatial calibration of Blaneye Criddle equation for calculating monthly ET_0 in south of Iran. Irrig Drain J 58(2):234–245

French A, Hunsaker D, Thorp K (2015) Remote sensing of evapotranspiration over cotton using the TSEB and METRIC energy balance models. Remote Sens Environ J 158:281–294

Hargreaves GH, Asce F, Allen G (2003) History end evaluation of Hargreaves evapotranspiration equation. Irrig Drain Eng J 129(1):53–63

Hernandez-Santana V, Fernández JE, Rodriguez-Dominguez CM, Romeroa R, Diaz-Espejo A (2016) The dynamics of radial sap flux density reflects changes in stomatal conductance in response to soil and air-water deficit. Agri for Meteorol 218–219:92–101

Irmak A, Allen RG, Kjaersgaard J, Huntington J, Kamble B, Trezza R, Ratcliffe I (2012) Operational remote sensing of ET and challenges, evapotranspiration - remote sensing and modeling, Dr. Ayse Irmak (Ed.), ISBN: 978–953–307–808–3, InTech, Available from: http://www.intechopen.com/books/evapotranspirat

ion-remote-sensing-and-modeling/operational-remotesensing-of-et-and-challenges. Accessed 14 Sep 2021

Jabloun M, Sahli A (2008) Evaluation of FAO-56 methodology for estimating reference evapotranspiration using limited climatic data. Application to Tunisia. Agr Water Manag J 95(6):707–715

Khoshravesh M, Gholami Sefidkouhi MA, Valipour M (2017) Estimation of reference evapotranspiration using multivariate fractional polynomial, Bayesian regression, and robust regression models in three arid environments. Appl Water Sci 7:1911–1922

Landeras G, Bekoe E, Ampofo J, Logah F, Diop M, Cisse M, Shiri J (2018) New alternatives for reference evapotranspiration estimation in West Africa using limited weather data and ancillary data supply strategies. Theor Appl Climatol 132:701–716

Lian J, Huang M (2016) Comparison of three remote sensing based models to estimate evapotranspiration in an oasis desert region. Agr Water Manag J 165:153–162

López Bernal Á, García Tejera O, Vega VA, Hidalgo JC, Testi L, Orgaz F, Villalobos FJ (2015) Using sap flow measurements to estimate net assimilation in olive trees under different irrigation regimes. Irrig Sci 33:357–366

Maeda E, Wibreg D, Pellikka P (2011) Estimating reference evapotranspiration using remote sensing and empirical models in a region with limited ground data availability in Kenya. Appl Geogr 31:251–258

Martinez CJ, Thepadia M (2010) Estimating reference evapotranspiration with minimum data in Florida. Irrig Drain Eng 136:494–501

Ma Y, Liua S, Song L, Xua Z, Liud Y, Xua T, Zhu Z (2018) Estimation of daily evapotranspiration and irrigation water efficiency at a Landsat-like scale for an arid irrigation area using multi-source remote sensing data. Remote Sens Environ J 216:715–734

Mahmoud S, Gan T (2019) Irrigation water management in arid regions of Middle East: assessing spatio-temporal variation of actual evapotranspiration through remote sensing techniques and meteorlogical data. Agr Water Manag J 212:35–47

Masmoudi-Charfi C, Habaieb H (2014) Rainfall distribution functions for irrigation scheduling: calculation procedures following site of olive (Olea europaea L.) cultivation and growing periods. Amer J Plant Sci 5:2094–2133

Melaouhi A, Baraza E, Escalona J, El-Aououad H, Mahjoub I, Bchir A, Braham M, Bota J (2021) Physiological and biochemical responses to water deficit and recovery of two olive cultivars (*Olea europaea L., Arbequina and Empeltre cvs*) under Mediterranean conditions. Theor Exper Plant Physiol J. https://doi.org/10.1007/s40626-021-00219-9

M'nassri S, Dridi L, Schäfer G, Hachicha M, Majdoub R (2019) Groundwater salinity in a semi-arid region of centrak eastern Tunisia: insights from multivariate statistical techniques and geostatistican modelling. Environ Earth Sci J 78:288

Nyenjie P, Batelaan O (2009) Estimating the efects of climate change on groundwater recharge and basefow in the upper Ssezibwa catchment. Ugenda Hydrol Sci J 54(4):713–726

Numata I, Khand K, Kjaersgaard J, Cochrane MA, Silva SS (2017) Evaluation of Landsat-based METRIC modeling to provide high-spatial resolution evapotranspiration estimates for Amazonian forests. Remote Sens 9(1):46

Paredes P, Rodrigues GC (2010) Necessidades de água para a rega de milho em Portugal Continental considerando condições de seca. In: Pereira LS, Mexia JT, Pires CAL (eds) Gestão do risco em secas: métodos, tecnologias e desafíos. Colibri e CEER, Lisboa, pp 301–320

Paredes P, Pereira LS, Almorox J, Darouich H (2020) Reference grass evapotranspiration with reduced data sets: Parameterization of the FAO Penman-Monteith temperature approach and the Hargeaves-Samani equation using local climatic variables. Agr Water Manag J. 240:106210

Ortega-Salazar S, Ortega-Farias S, Kilic A, Allen R (2021) Performance of the METRIC model for mapping energy balance components and actual evapotranspiration over a super intensive drip-irrigated olive orchard. Agr Water Manag J 251:106861

Pereira LS, Paredes P, Jovanovic N (2020) Soil water balance models for determining crop water and irrigation requirements and irrigation scheduling focusing on the FAO56 method and the dual Kc approach. Agr Water Manag J 241(1):106357

Pôças I, Paço TA, Cunha M, Andrade JA, Silvestre J, Sousa A, Santos FL, Pereira LS, Allen RG (2014) Satellite-based evapotranspiration of a super-intensive olive orchard: application of METRIC algorithms. Biosyst Eng 128:69–81

Popova Z, Kercheva M, Pereira LS (2006) Validation of the FAO methodology for computing ET0 with missing climatic data. Appl South Bulgaria Irri Drain 55:201–215. https://doi.org/10.1002/ird.228

Priestley CHB, Taylor RJ (1972) On the assessment of surface heat flux and evaporation using large-scale parameters. Mon Weather Rev 100:81–92

Razieia T, Pereira LS (2013) Reference estimation of ET0 with Hargreaves-Samani and FAO-PM temperature methods for a wide range of climates in Iran. Agr Water Manag 121:1–18. https://doi.org/10.1016/j.agwat.2012.12.019

Saadi S (2018) Spatial estimation of actual evapotranspiration and irrigation volumes using water and energy balance models forced by optical remote sensing data (VIS / NIR/ TIR). PhD Thesis, Université de Toulouse France. P. 294

Sumner D, Jacobs JM (2005) Utility of Penman-Monteith, Priestley–Taylor, reference evapotranspiration, and pan evaporation methods to estimate pasture evapotranspiration. Hydrol J 308:81–104

Tabari H (2010) Evaluation of reference crop evapotranspiration equations in various climates. Water Res Manag 24:2311–2337

Tasumi M (2019) Estimating evapotranspiration using METRIC model and Landsat data for better understandings of regional hydrology in the western Urmia Lake Basin. Agr Water Manag. 226:105805

Temesgen B, Eching S, Davidoff B, Frame K (2005) Comparison of some reference evapotranspiration equations for California. Irrig Drain Eng 13:73–84. https://doi.org/10.1061/(ASCE)0733-9437

Todorovic M, Karic B, Pereira LS (2013) Reference evapotranspiration estimate with limited weather data across a range of Mediterranean climates. Hydrol J 481:166–176. https://doi.org/10.1016/j.jhydrol.2012.12.034

Valipour M (2017) Analysis of potential evapotranspiration using limited weather data. Appl Water Sci 7:187–197. https://doi.org/10.1007/s13201-014-0234-2

Wrachien DD, Mambretti S (2015) Irrigation and drainage systems in flood-prone areas: The role of mathematical models. Austin J Irrig 1(1):1002

Xue J, Balic K, Light S, Hessels T, Kisekka I (2020) Evaluation of remote sensing-based evapotranspiration models against surface renewal in almonds, tomatoes and maize. Agr Water Manag J 238:106228

Xiaoying L, Erda L (2005) Performance of the Priestley-Taylor equation in the semiarid climate of North China. Agr Water Manag J 71(1):1–17. https://doi.org/10.1016/j.agwat.2004.07.007

Yannopoulos SI, Lyberatos G, Theodossiou N, Li W, Valipour M, Tamburrino A, Angelakis AN (2015) Evolution of water lifting devices (pumps) over the centuries worldwide. Water 7(9):5031–5060. https://doi.org/10.3390/w7095031